

---

# Output Based Grid Adaptation for Viscous Flow

Julie C. Andren<sup>1</sup> and Michael A. Park<sup>2</sup>

<sup>1</sup> Massachusetts Institute of Technology, [jandren@mit.edu](mailto:jandren@mit.edu)

<sup>2</sup> NASA Langley Research Center, Computational AeroSciences Branch,  
[Mike.Park@NASA.gov](mailto:Mike.Park@NASA.gov)

## 1 Introduction

Output (adjoint) based adaptation is a method that has been used to automate the unstructured grid generation task of inviscid [3] and two-dimensional (2D) turbulent [6, 7] flow simulation. This project challenges existing three dimensional (3D) techniques to produce strongly anisotropic grids for modeling the boundary layer on a flat plate. Elements with large face angles can cause difficulties for the diffusion operator employed in this study [1], so a range of Reynolds numbers are explored to quantify the accuracy of the solutions on the output adapted grids. Laminar and turbulent flows are simulated on an extruded flat plate to exercise the 3D algorithm on a case with a known solution. Regular, fully adapted, and hybrid unstructured tetrahedral grids are used to examine the ability of different grid constructions to reproduce Blasius or empirically derived velocity profiles. The hybrid approach retained the original regular tetrahedral grid near the flat plate and adapted the grid outside of this region. This approach produced similar velocity profiles to the regular grids and better results than the fully adaptive cases for the highest Reynolds number cases.

## 2 Output-Based Adaptation

The output adaptive capability of the FUN3D suite of computational fluid dynamics tools is utilized. The FUN3D website <http://fun3d.larc.nasa.gov> contains a user manual as well as an extensive list of references. The embedded-grid error estimation procedure [2, 6, 7] for the output of drag on the flat plate is combined with the Mach Hessian to produce an anisotropic metric. Parallel 3D grid mechanics [3, 4] that include enrichment, coarsening, node movement, and element connectivity changes utilize this metric.

### 3 Results

The grid on one symmetry plane of the 3D extruded flat plate domain is shown in Fig. 1. Flow is from left to right. The original grid used for full adaptation, Fig. 1(a), has a coarse isotropic grid spacing with refinement at the leading edge singularity of the flat plate. This initial spacing is not suitable for laminar flow simulation and is intended to stress the adaptive process. The regular grid is shown in Fig. 1(b). It has a sinusoidal spacing along the plate to provide clustering near the leading edge singularity. A geometric growth of grid spacing is applied in the direction normal to the plate. This regular grid is also used as the initial grid for hybrid adaptation where the grid is held constant or frozen in the region where  $\eta \leq 1$  near the flat plate, where  $\eta = z\sqrt{Re}$ ,  $z$  is the distance normal to the plate, and  $Re$  is the Reynolds number.

The final grid for the fully adapted case is shown in Fig. 1(c). A detail of the boundary layer region is shown in Fig. 1(e). The vertical axis of Fig. 1(e) is stretched by a factor of ten to improve visualization of the high aspect ratio grid. The final grid for the hybrid case is shown in Fig. 1(d) and Fig. 1(f) with an expanded vertical axis. Adaptation refines the elements near the leading edge and in the boundary layer. These grids are used to simulate laminar flow at a  $Re = 1,000,000$ . The initial grids are simple and easy to manually generate for this case with trivial geometry, but can be difficult for more general problems. The boundary layer detail clearly shows the stretched high aspect ratio cells.

The regular and fully adapted grid laminar boundary layer velocity profiles for  $Re = 100,000$  and  $Re = 1,000,000$  are shown in Fig. 2. Simulation results are plotted with red circles to compare with the blue line of the Blasius solution. The velocity is sampled across the span of the 3D extruded domain, so any spanwise variation in velocity is seen as red circle scatter. Profiles produced by the regular grid closely fit the Blasius solution for both  $Re$  cases, as shown in Fig. 2(a) and Fig. 2(b). The full adaptation approach is able to produce a velocity profile that matches the Blasius solution for the  $Re = 100,000$  case, Fig. 2(c). However, the  $Re = 1,000,000$  full adaptation case was not able to produce a suitable grid. A significant variability in the velocity across the span of the flat plate results in the scatter of the Figure 2(d) circle symbols. The scalar output adaptation request for the  $Re = 1,000,000$  full adaptation case is shown in Fig. 3. The adaptation parameter is less than one in the boundary layer, indicating that grid refinement is being requested. However, the existing grid mechanics are unable to satisfy it because of grid quality constraints built into the adaptation mechanics.

The hybrid adaptive grid approach is employed to produce the velocity profiles in Fig. 4. Figure 4(a) is a laminar flat plate at  $Re = 1,000,000$  and Fig. 4(b) is a turbulent flat plate at  $Re = 10,000,000$ . The one equation Spalart-Allmaras turbulence model [5] is employed for the turbulent calculation. The  $Re = 1,000,000$  laminar hybrid case, Fig. 4(a), produced an improved

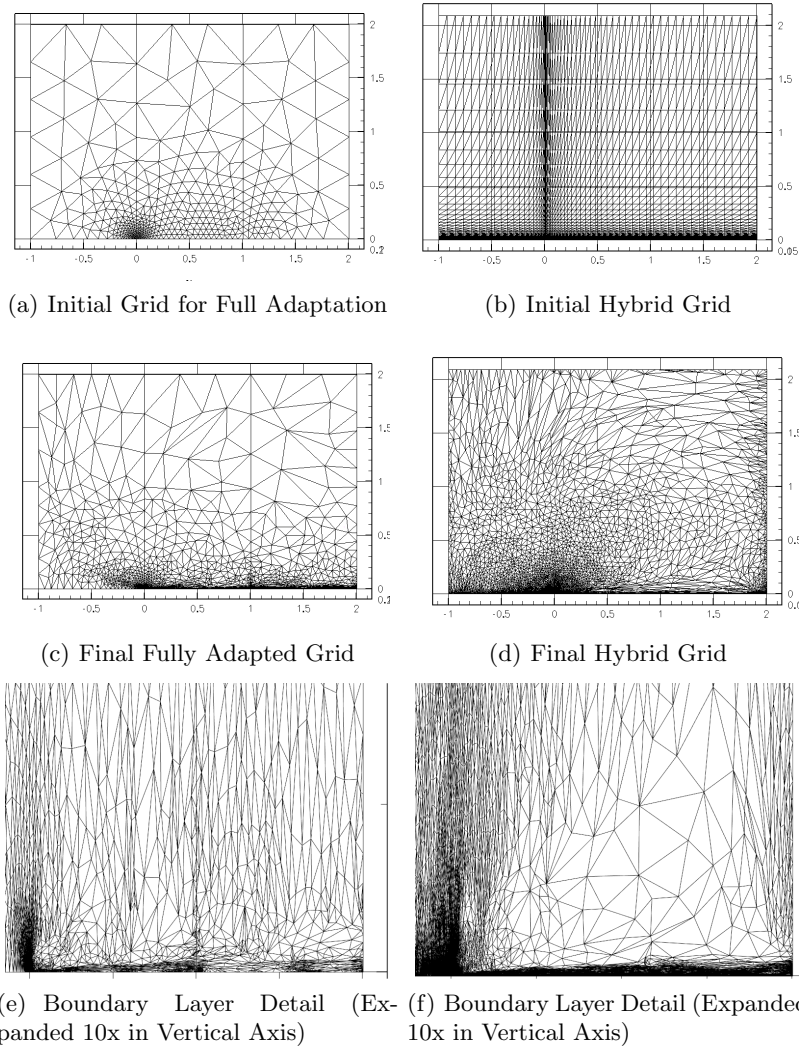


**Fig. 1.** Initial, Final, and Boundary Layer Grids for Full Adaptation and Hybrid Methods, Laminar,  $Re = 1,000,000$ .

velocity profile as compared to the regular, Fig. 2(b), and full adaptation, Fig. 2(d), grid solutions. The turbulent fully adaptive method (not shown) failed to complete the adaptive process when started with the coarse initial isotropic grid, Fig. 1(a). The turbulent hybrid case matched the expected blue asymptotic curves for both the sublayer and log layers. The grid was frozen for points in the sublayer and most of the log layer,  $y^+ < 300$ .

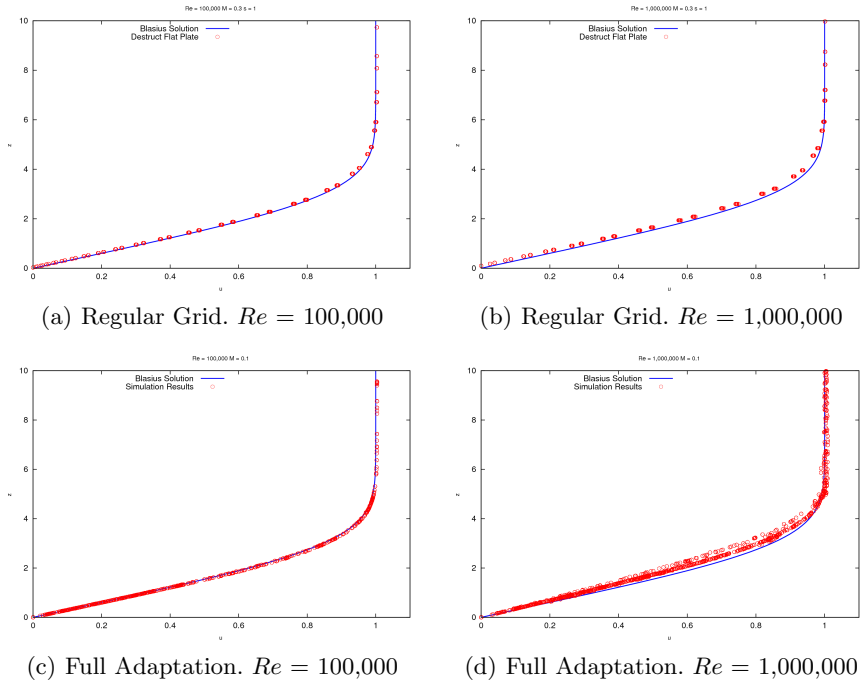


**Fig. 2.** Velocity Profiles for Laminar Boundary Layer

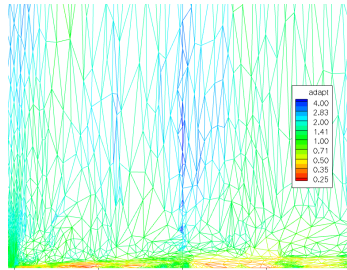


**Fig. 3.** Drag Output Adaptation Parameter for  $Re = 1,000,000$  Laminar Case (Expanded 10x in Vertical Axis).

## 4 Summary

Grid adaptation for 3D viscous flows is studied by comparing three tetrahedral grid generation techniques: regular, full grid adaptation, and hybrid grid adaptation. Full adaptation is successful for the lower  $Re$  case, but is currently unable to accurately refine cells in boundary layers with the greater  $Re$  when coarse isotropic initial grids are employed. The hybrid approach does not alter the regular cells near a solid wall while adapting all other cells. Mod-

eling viscous flow using a hybrid grid eliminates the spanwise scatter of the fully adapted grid and yields similar, if not more accurate, results to those produced when using regular grids. The hybrid adaptation technique also accurately predicted a turbulent boundary layer with a one equation turbulence model. This hybrid approach maintains the solution in the lowest portion of the boundary layer using regular grids and adaptation away from the body.

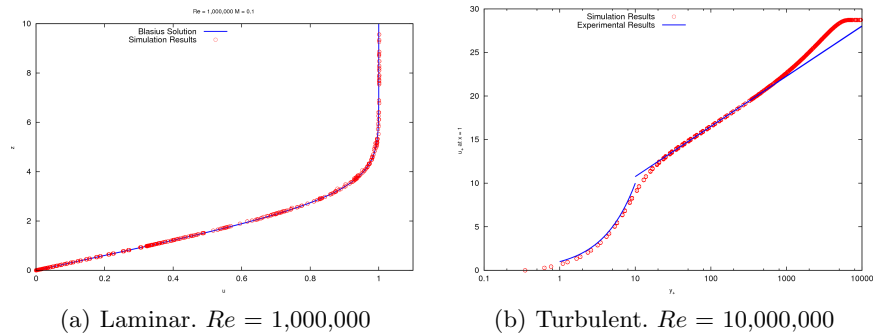


Fig. 4. Velocity Profiles Using Hybrid Grid Generation

## References

1. B. Diskin, J. L. Thomas, E. J. Nielsen, H. Nishikawa, and J. A. White. Comparison of node-centered and cell-centered unstructured finite-volume discretizations. part i: viscous fluxes. AIAA Paper 2009–597, 2009.
2. M. A. Park. Three-dimensional turbulent rans adjoint-based error correction. AIAA Paper 2003–3849, 2003.
3. M. A. Park. *Anisotropic Output-Based Adaptation with Tetrahedral Cut Cells for Compressible Flows*. PhD thesis, Massachusetts Institute of Technology, Sept. 2008.
4. M. A. Park and D. Darmofal. Parallel anisotropic tetrahedral adaptation. AIAA Paper 2008–917, 2008.
5. P. R. Spalart and S. R. Allmaras. A one-equation turbulence model for aerodynamic flows. *La Recherche Aeronautique*, (1):5–21, 1994.
6. D. A. Venditti. *Grid Adaptation for Functional Outputs of Compressible Flow Simulations*. PhD thesis, Massachusetts Institute of Technology, 2002.
7. D. A. Venditti and D. L. Darmofal. Anisotropic grid adaptation for functional outputs: Application to two-dimensional viscous flows. *Journal Computational Physics*, 187:22–46, 2003.